Preprints of the 21st IFAC World Congress (Virtual)
Berlin, Germany, July 12-17, 2020

Performance Optimization Methodology for Discrete-Time Sliding Mode Control in Industrial Servo Systems Under Control Input Saturation and Disturbance

Ji-Seok Han*, Tae-Ho Oh*, Young-Seok Kim*, Hyun-Taek Lim*, Dae-Young Yang*, Sang-Hoon Lee, and Dong-Il "Dan" Cho***

**ASRI/ISRC, Department of Electrical and Computer Engineering, Seoul National University, Seoul, 08826 Korea (e-mail: dicho@snu.ac.kr)*
*** RS Automation Co., Ltd., Gyeonggi-do, 17709 Korea (e-mail: shlee@rsautomation.co.kr)*

Abstract: This paper presents a performance optimization methodology for the discrete-time sliding mode control (SMC) with the decoupled disturbance compensator (DDC) and the auxiliary state (AS) for an industrial position control system under control input saturation and disturbance. The discrete-time SMC with DDC and AS (SDA) method prevents windup phenomena in the switching function and the disturbance estimation error. Therefore, it provides robust performance under control input saturation, disturbances, as well as parametric uncertainties. However, it is difficult to relate several design parameters to the desired performance. In this paper, a systematical design framework for the discrete-time SDA method is developed. Based on the phase portrait of the error state, the error can be made to converge to zero with a fast speed and less oscillation under control input saturation by an offline tuning process. An optimization process is performed in terms of the peak value of the control input. Both numerical simulations and experimental results show the effectiveness of the developed tuning methodology for the discrete-time SDA method.

Keywords: Discrete-time Sliding Mode Control, Decoupled Disturbance Compensator, Control Input Saturation, Auxiliary State.

1. INTRODUCTION

In many practical control systems, a precise motion control with a fast response under disturbances has been considered as an important issue to control engineers. In industrial servo systems, there are various machines that are connected with servo motors. These machines require high-performance, robust controllers because there are uncertainties in modelling errors and external disturbances (Bahn *et al.*, 2017; Yoon *et al.*, 2017). There has been much research to obtain robust performance in servo systems. Lu *et al.* (2018) designed an uncertainty and disturbance estimator-based controller for trajectory tracking of a quadrotor to deal with highly nonlinear system dynamics. Zhang *et al.* (2018) developed a cascade active disturbance rejection control method for a quadrotor unmanned aerial vehicle to compensate for internal and external uncertainties. Nguyen *et al.* (2018) proposed a backstepping adaptive fuzzy sliding mode control for an electrohydraulic series elastic manipulator to deal with chattering phenomenon and uncertainties in the system. In addition, the sliding mode control method has been widely implemented to obtain robust performance under system uncertainties for automotive engines (Cho and Hedrick, 1988; Cho and Oh, 1993), magnetic levitation systems (Cho *et al.*, 1993), industrial servo systems (Eun *et al.*, 1999; Eun and Cho, 1999; Kim *et al.*, 2000; Milosavljevic *et al.*, 2000; Bahn *et al.*, 2014; Han *et al.,* 2017, 2018), piezoelectric nanopositioning systems (Wang and Xu, 2018), and elastic actuators (Yin *et al.*, 2018).

Meanwhile, actuator saturation prevails in nearly all practical applications when the control command is applied beyond the physical limits of actuators. Control input saturation can cause severe problems such as large overshoot, oscillations, and even instability. Therefore, considering input saturation as well as disturbance rejection is essential. Huang *et al.* (2013) proposed an adaptive parameter tuning method which computes the bounded torque input in advance to deal with control input saturation. Zhou *et al.* (2019) developed a finite-time attitude control method for a quadrotor system in the presence of input saturation and time-varying disturbance. An enhanced decoupled disturbance compensator was developed for a discrete-time sliding mode control, which preserves the disturbance estimation error dynamics under input saturation (Han *et al.*, 2016). Disturbance observers and auxiliary systems have been widely utilized for dealing with both disturbances and input saturation. Du *et al.* (2016) designed a disturbance observer and an auxiliary system for ships to deal with unknown time-varying disturbance and input saturation. The discrete-time SDA method was proposed for a high-precision servo system (Han *et al.*, 2020), which preserves the original disturbance estimation error dynamics as well as the sliding mode dynamics even in the presence of control input saturation and disturbance by applying a new auxiliary state. However, additional oscillations or slow convergence of the position error can appear when the control parameters are not appropriately selected under unexpected saturation environments. However,

because there are many control parameters, selecting appropriate gains is very difficult.

Therefore, an optimized design methodology for the discrete-time SDA method for a servo system is proposed in this paper. Especially, the error dynamics and the phase portraits during deceleration will be considered in detail. In a first step, the mover of the servo system is driven once, and the maximum position error is measured during deceleration with an arbitrary gain of the auxiliary state under control input saturation. In the next step, the optimized gain of the auxiliary state is calculated offline in a way that the peak value of the control input stays within the bounds of the actuator limit. This design methodology provides a simple and effective tuning guideline of the discrete-time SDA method under both disturbances and control input saturation. The numerical simulations and experiments are performed to demonstrate the effectiveness of the proposed tuning methodology.

The rest of the paper is organized as follows. Section 2 formulates the problem of the position control system by using the discrete-time SDA method under control input saturation. In section 3, the proposed design methodology of the discrete-time SDA method is introduced with numerical simulation results. In section 4, experiments are performed on a servo system with a disc payload to show the robust performance under disturbance and control input saturation.

2. PROBLEM FORMULATION

Consider the discrete servo system model with control input saturation.

$$\mathbf{x}_{k+1} = \mathbf{A}\mathbf{x}_k + \mathbf{B}u^{\lim}\mathrm{sat}\left(\frac{u_k}{u^{\lim}}\right) + \mathbf{B}f_k, \tag{1}$$

where $\mathbf{x}_k = \begin{bmatrix}\theta_k & \omega_k\end{bmatrix}^T$ is the state variable, θ_k is the angular position, ω_k is the angular velocity, u_k is the control input, $u^{\lim}$ is the positive limit for control input, $\mathbf{A} = \begin{bmatrix}1 & T\\ 0 & 1\end{bmatrix}$ is the system matrix, T is the sampling period, $\mathbf{B} = \begin{bmatrix}k_t T^2/(2J) & k_t T/J\end{bmatrix}^T$ is the input matrix, k_t is the torque constant, J is the inertia of the system, and f_k is the disturbance which is comprised of the model uncertainties and external disturbance. $\mathrm{sat}(u_k)$ is defined as follows:

$$\mathrm{sat}(u_k) = \begin{cases}\dfrac{u_k}{|u_k|} & \text{if } |u_k| > 1\\ u_k & \text{otherwise.}\end{cases} \tag{2}$$

Han *et al*. (2020) proposed the following auxiliary state and the switching function for the discrete-time sliding mode controller.

$$z_k = \alpha z_{k-1} + (\mathbf{GB})\Delta u_{k-1}, \tag{3}$$

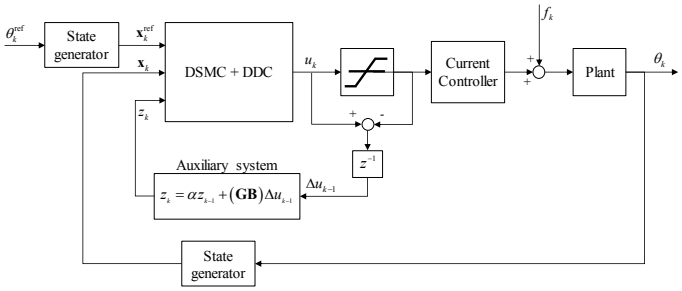

Fig. 1. Structure of discrete-time SDA.

$$\sigma_k = \mathbf{G}\mathbf{e}_k + z_k, \tag{4}$$

where z_k is the auxiliary state, α is the gain parameter of the auxiliary system, $\Delta u_k = u_k - u^{\lim}\mathrm{sat}\left(\frac{u_k}{u^{\lim}}\right)$ is the difference between the controller output and the actual control input to the plant, $\mathbf{e}_k = \mathbf{x}_k - \mathbf{x}_k^{\mathrm{ref}} = \begin{bmatrix}\tilde{\theta}_k & \tilde{\omega}_k\end{bmatrix}^T$ is the error state, $\mathbf{x}_k^{\mathrm{ref}} = \begin{bmatrix}\theta_k^{\mathrm{ref}} & \omega_k^{\mathrm{ref}}\end{bmatrix}^T$ is the reference vector, $\tilde{\theta}_k = \theta_k - \theta_k^{\mathrm{ref}}$ is the position error, $\tilde{\omega}_k = \omega_k - \omega_k^{\mathrm{ref}}$ is the velocity error, and $\mathbf{G} = \begin{bmatrix}g_1 & g_2\end{bmatrix}$ is the gain vector. α should be selected by $0 < \alpha < 1$. Then the discrete-time SDA control law can be expressed as follows:

$$u_k = -\hat{f}_k + (\mathbf{GB})^{-1}\left[\mathbf{G}\mathbf{x}_{k+1}^{\mathrm{ref}} - \mathbf{G}\mathbf{A}\mathbf{x}_k - \alpha z_k + q\sigma_k - \eta\ \mathrm{sat}\left(\frac{\sigma_k}{\phi}\right)\right], \tag{5}$$

$$\hat{f}_k = \hat{f}_{k-1} + g(\mathbf{GB})^{-1}\left[\sigma_k - q\sigma_{k-1} + \eta\ \mathrm{sat}\left(\frac{\sigma_{k-1}}{\phi}\right)\right], \tag{6}$$

where q is the gain of the sliding mode dynamics, η is the gain of the discontinuous control part, ϕ is the boundary layer thickness of quasi-sliding mode, $\hat{f}_k$ is the estimated disturbance, and g is the gain of the DDC. To reduce the chattering effect, a saturation function is used in the discontinuous control part. The overall structure of the discrete-time SDA method is depicted in Fig. 1. It was proved that the following sliding mode dynamics and disturbance estimation error dynamics are satisfied under disturbance and control input saturation (Han *et al*., 2020).

$$\sigma_{k+1} = q\sigma_k - \eta\mathrm{sat}\left(\frac{\sigma_k}{\phi}\right) + \mathbf{GB}\tilde{f}_k, \tag{7}$$

$$\tilde{f}_{k+1} = (1-g)\tilde{f}_k + f_{k+1} - f_k, \tag{8}$$

where $\tilde{f}_k = f_k - \hat{f}_k$ is the disturbance estimation error.

The discrete-time SDA method is highly efficient for servo control systems due to the excellent tracking performance and the stability under disturbance and control input saturation.

3. PROPOSED DESIGN METHODOLOGY

The auxiliary state in the sliding mode controller plays an important role in that it governs the dominant dynamics under control input saturation. Therefore, adjusting the parameter of the auxiliary state, α, is an important issue in practice. If α is closer to one, the error dynamics have less oscillations, but the convergence speed decreases. On the other hand, if α is closer to zero, the convergence speed increases, but additional oscillations can occur. It is hard to design the control parameters in practical systems to obtain a fast convergence and less oscillation under control input saturation. Fig. 2(a) and 2(b) show the simulation results for $\alpha = 0.92$ and $\alpha = 0.995$, respectively. The other parameters of discrete-time SDA are $\mathbf{G} = \begin{bmatrix} 298 & 1 \end{bmatrix}$, $q = 0.982$, $\eta = 0.183$, $g = 0.0366$, and $\phi = 10$. The target reference position is 10 turns, the maximum reference velocity is 2,000 rev/min, and the acceleration and deceleration times are both 20 ms. During the deceleration in Fig. 2(a), there is a second peak in the position error, which is undesirable. During the deceleration in Fig. 2(b), there is no second peak in the position error, but the convergence speed is too slow. Therefore, the gain α should be larger than 0.92 and less than 0.995. Therefore, a manual tuning procedure is required to obtain the desired performance.

In this paper, an optimized design methodology for the discrete-time SDA method is presented. Figs. 3(a) and 3(b) are the phase portraits for the error vector during the deceleration of the simulation results in Figs. 2(a) and 2(b), respectively. The blue upper, middle and lower lines are the sets where the control input has the values of $u_k = -u^{\lim}$, $u_k = 0$, and $u_k = u^{\lim}$, respectively. The red line is the stable node which is only guaranteed in the set $\left\{ \mathbf{e}_k : |u_k| \le u^{\lim}, |\sigma_k| < \phi \right\}$. First, the maximum position error, $\begin{bmatrix} \tilde{\theta}_{\max} & 0 \end{bmatrix}^T$, is measured which is depicted by the green point in Fig. 3. The arbitrary gain parameters including α are allowed in the first driving test. In the region beyond the blue upper line, the error dynamics can be represented as follows:

$$\mathbf{e}_{k+1} = \mathbf{A}\mathbf{e}_k - \mathbf{B}u^{\lim}, \tag{9}$$

where $|\tilde{f}_k| \approx 0$ and $|\sigma_k| \approx 0$ are assumed. Then the following parabolic relationship between the position error and the velocity error is satisfied.

$$\begin{bmatrix} \tilde{\theta}_{k+1} \\ \tilde{\omega}_{k+1} \end{bmatrix} = \begin{bmatrix} 1 & T \\ 0 & 1 \end{bmatrix} \begin{bmatrix} \tilde{\theta}_k \\ \tilde{\omega}_k \end{bmatrix} - \begin{bmatrix} \frac{T}{2} \\ 1 \end{bmatrix} c, \tag{10}$$

$$\tilde{\theta}_k - \tilde{\theta}_0 = -\frac{T}{2c}\left(\tilde{\omega}_k^2 - \tilde{\omega}_0^2 \right), \tag{11}$$

where $c = \frac{k_t T}{J} u^{\lim}$. The parabolic trajectory is shown in Fig. 3. When the error enters the region inside the blue upper and the blue lower lines, the error attempts to converge to the stable node as shown in Fig. 3(b). However, the error can escape the region when $u^{\lim}$ or α are low as shown in Fig. 3(a). The error trajectory during deceleration depends on the motor parameters and control limits. Also, the blue lines depend on

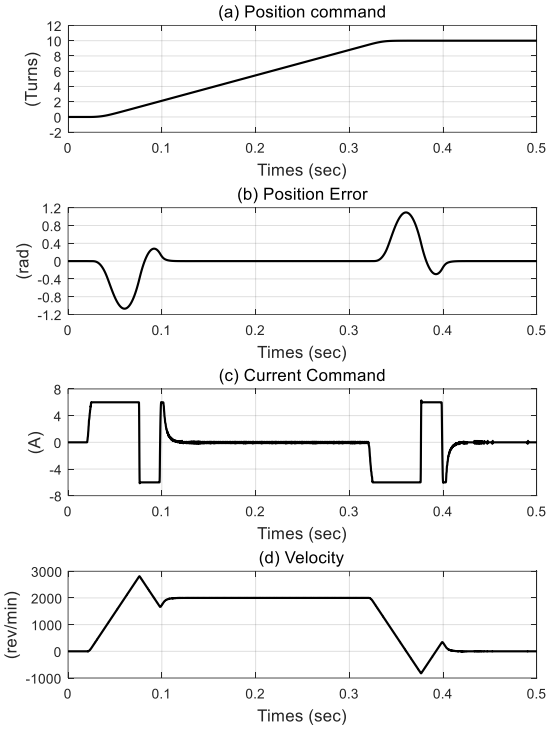

(a) α=0.92

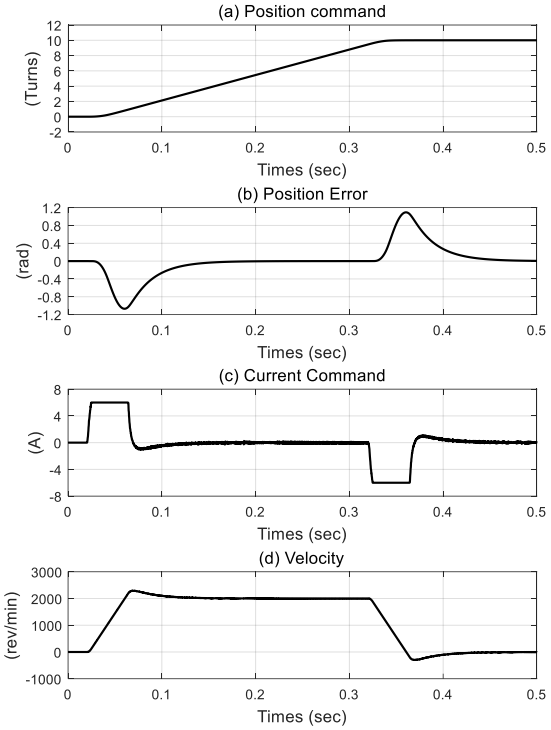

(b) α=0.995

Fig. 2. Simulation results.

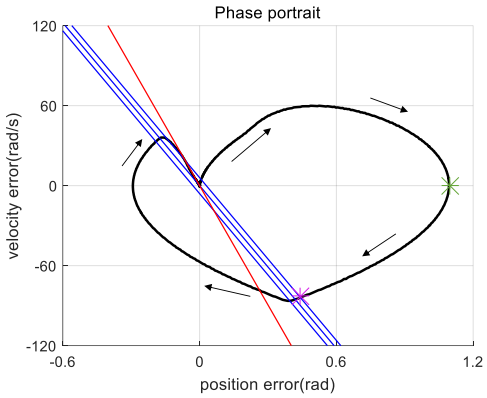

(a) α=0.92

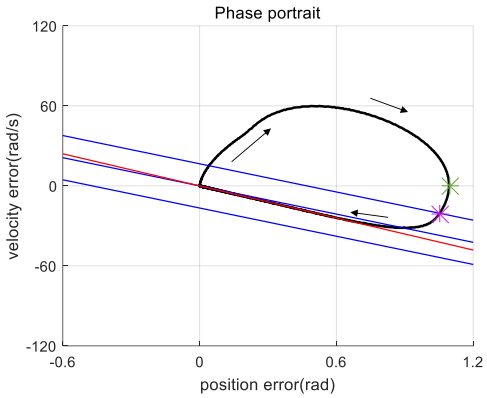

(b) α=0.995

Fig. 3. Phase portraits.

the parameters of the discrete-time SDA method. The set of the blue upper line satisfies the following equation.

$$u_k = -\mathbf{P}\mathbf{e}_k = -p_1\tilde{\theta}_k - p_2\tilde{\omega}_k = -u^{\lim}, \tag{12}$$

where $\mathbf{P} = \begin{bmatrix} p_1 & p_2 \end{bmatrix} = (\mathbf{GB})^{-1}\mathbf{G}(\mathbf{A} - \alpha_0\mathbf{I}_{2\times 2})$, and α_0 is the initial gain parameter of the auxiliary state in the first driving test. By equating (11), (12) and $\begin{bmatrix} \tilde{\theta}_0 & \tilde{\omega}_0 \end{bmatrix}^T = \begin{bmatrix} \tilde{\theta}_{\max} & 0 \end{bmatrix}^T$, the purple point, $\begin{bmatrix} \tilde{\theta}_k & \tilde{\omega}_k \end{bmatrix}^T = \begin{bmatrix} \tilde{\theta}_s & \tilde{\omega}_s \end{bmatrix}^T$, can be obtained. In the region inside the blue upper and the blue lower lines, the error should not escape this region not to generate additional control input saturation. In addition, the maximum control input should be large but less than the control limit, $u^{\lim}$, to converge to zero with high speed. It means that the optimized trajectory of the error which starts from the purple point should touch the lower blue line. Therefore, the following equations should be satisfied:

$$\mathbf{e}_{k+1} = (\mathbf{A} - \mathbf{BP})\mathbf{e}_k, \mathbf{e}_0 = \begin{bmatrix} \tilde{\theta}_s & \tilde{\omega}_s \end{bmatrix}^T, \tag{13}$$

$$u_k = -\mathbf{P}\mathbf{e}_k = -p_1\tilde{\theta}_k - p_2\tilde{\omega}_k = u^{\lim}. \tag{14}$$

In conclusion, the proposed design methodology is summarized as follows:

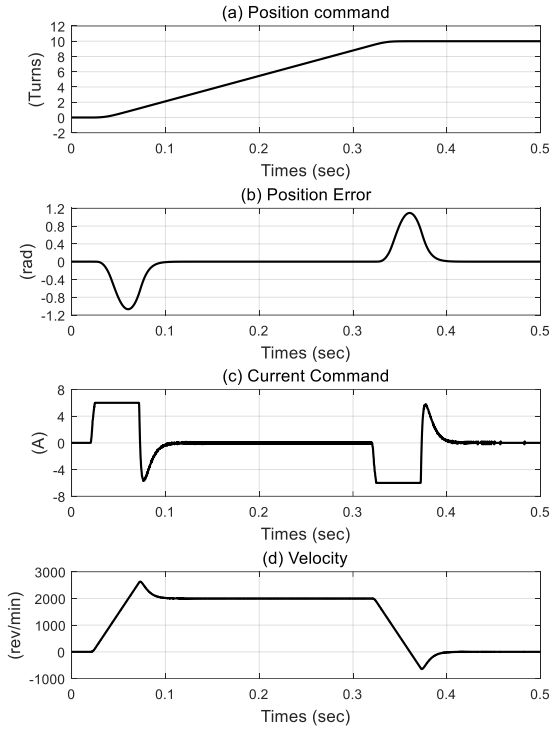

Fig. 4. Simulation results (α=0.98).

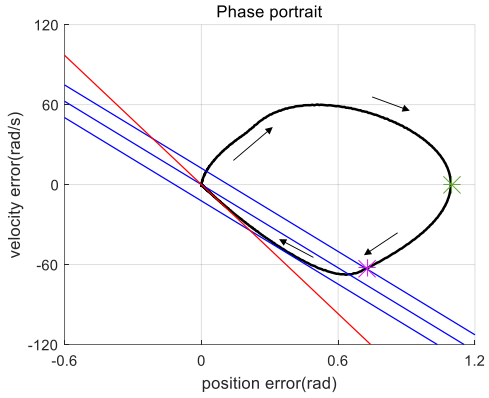

Fig. 5. Phase portrait (α=0.98).

Step 1. For an arbitrary initial value of α_0, drive the system once, and measure the maximum position error (the green point in Fig. 3).

Step 2. With the given system parameters, find the purple point in Fig. 3 using (11), (12) and the green point.

Step 3. Find the expected maximum control input using (13) and (14).

Step 4. If the maximum control input is less than $u^{\lim}$, decrease a small amount of α and go to step 2. If the maximum control input is larger than $u^{\lim}$, increase a small amount of α and go to step 2. If the maximum control input is near $u^{\lim}$, terminate the tuning procedure. The final value of α is the optimized value of the discrete-time SDA method.

Figs. 4 and 5 are the simulation results and the phase portrait, respectively, after the proposed design procedure is done.

The optimized α is 0.98. The position error in Fig. 4 converges to zero faster than the case of α=0.995 as shown in Fig. 2(b). In addition, there is no additional oscillation as shown in Fig. 4. On the other hand, there is the additional oscillation in the case of α=0.92 as shown in Fig. 2(a). Therefore, the proposed design methodology provides desired control performances for the discrete-time SDA method.

Remark 1. When the control parameters, system parameters, and reference profiles are changed, the proposed tuning procedure should be performed again.

Remark 2. The proposed design methodology is performed offline, and thus the computational complexity poses no issue.

4. EXPERIMENTS

Experiments are performed on an AC servo motor (RS Automation, Korea) to show the practicability of the developed methodology. The controller is implemented in a digital signal processor of 400 W servo drive (RS Automation, Korea). A disc payload is added whose inertia is 10 times larger than the rotor inertia to test under the control input saturation environments. The total inertia is $3.74\times10^{-4}\text{kg}\cdot\text{m}^2$ and the torque constant is $0.28\text{N}\cdot\text{m/A}$. The laboratory setup is shown in Fig. 6. The target reference position is 10 turns, the maximum reference velocity is 2,000 rev/min, and both the acceleration and deceleration times are 20 ms, which is shown in Fig. 7. The gain parameters are given as $\mathbf{G}=\begin{bmatrix}100 & 1\end{bmatrix}$, $q=0.99$, $\eta=0.3$, $g=0.03$, and $\phi=10$. The tacktime is measured, where the tacktime is the time interval from the end time of the reference position to the time when the position error is bounded within 3.83×10^{-4} radian. The black and blue lines in Fig. 8 are the experimental results when α is set as 0.9 and 0.996, respectively. In Fig. 8(c), control input saturation occurs twice during the deceleration in the black line, and an additional oscillation appears in the position error. In Fig. 8(a), there is no additional oscillation in the position error of the blue line during the deceleration, but the convergence speed is too slow. After applying the developed design methodology, the optimized α is set to be 0.99, and the experimental results are shown in the red line of Fig. 8. Compared to the previous cases, the desired performances can be obtained with less oscillation and the fast response. The experimental results are summarized in Table 1, which demonstrate the effectiveness of the proposed tuning methodology for the discrete-time SDA method.

Table 1. Experimental results during deceleration

	α=0.9	α=0.996	α=0.99
1st overshoot (rad)	3.28	3.28	3.26
2nd overshoot (rad)	0.80	0.00	0.00
Tacktime (ms)	160	196	132

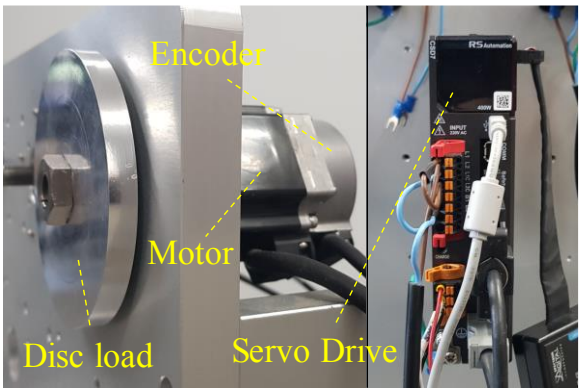

Fig. 6. Experimental setup.

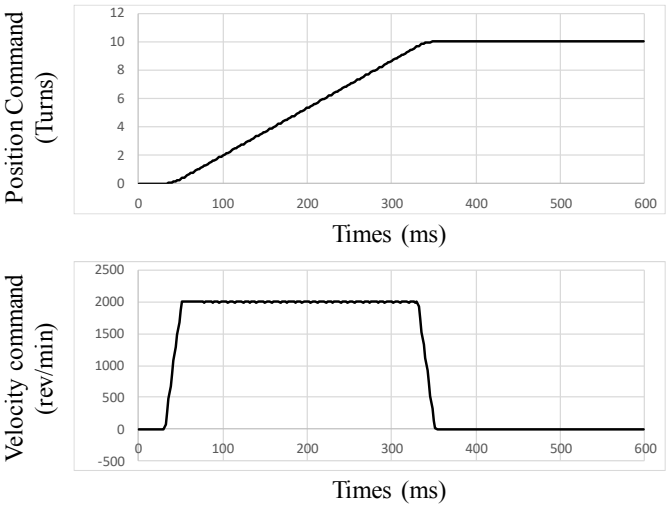

Fig. 7. Reference Profiles.

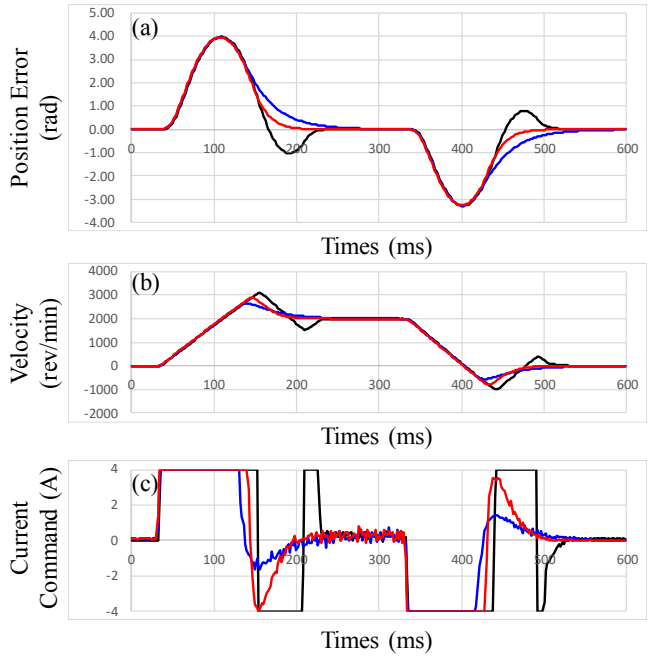

Fig. 8. Experimental results (black line: α=0.9, blue line: α=0.996, red line: α=0.99).

5. CONCLUSIONS

This paper designed a simple and effective design methodology for the discrete-time SDA method under control input saturation and disturbance. With the proposed optimization methodology, good position tracking performance with less oscillation and high convergence speed can be achieved even when input saturation occurs. Numerical simulations and experimental results showed the effectiveness of the designed tuning methodology.

ACKNOWLEDGMENT

This work was supported by the World Class 300 Project(R&D)(S2563339) of the Ministry of SMEs and Startups (Korea).

REFERENCES

Bahn, W., Kim, T., Lee, S., and Cho, D. (2017). Resonant frequency estimation for adaptive notch filters in industrial servo systems. *Mechatronics*, 41, 45–57.

Yoon, J. Bahn, W., Kim, T., Han, J., Lee, S., and Cho, D. (2017). Discrete derivative method for adaptive notch filter-based frequency estimators. *International Journal of Control, Automation and Systems*, 15 (2), 668–679.

Lu, Q., Ren, B., Parameswaran, S., and Zhong, Q. (2018). Uncertainty and disturbance estimator-based robust trajectory tracking control for a quadrotor in a global positioning system-denied environment, *J. Dyn. Sys,, Meas., Control*, 140 (3), 031001.

Zhang, Y., Chen, Z., Zhang, X., Sun, Q., and Sun, M. (2018). A novel control scheme for quadrotor UAV based upon active disturbance rejection control, *Aerospace Science and Technology*, 79, 601–609.

Nguyen, M., Tran, D. and Ahn, K. (2018). Robust position and vibration control of an electrohydraulic series elastic manipulator against disturbance generated by a variable stiffness actuator, *Mechatronics*, 52, 22–35.

Cho, D., and Hedrick, J. (1988). A nonlinear controller design method for fuel-injected automotive engines. *Journal of Engineering for Gas Turbines and Power*, 110 (3), 313–320.

Cho, D., Kato, Y. and Spilman, D. (1993). Sliding mode and classical controllers in magnetic levitation systems. *IEEE Control Systems Magazine*, 13 (1), 42–48.

Cho, D. and Oh, H. (1993). Variable structure control method for fuel-injected systems. *Journal of Dynamic Systems, Measurement, and Control*, 115 (3), 475–481.

Eun, Y., Kim, K., Kim, J., and Cho, D. (1999). Discrete-time variable structure controller with a decoupled disturbance compensator and its application to a CNC servomechanism. *IEEE Trans. Control Sys. Technol.*, 7 (4), 414–423.

Eun, Y. and Cho, D. (1999). Robustness of multivariable discrete-time variable structure control. *International Journal of Control*, 72 (12), 1106–1115.

Kim, J., Oh, S., Cho, D., and Hedrick, J. (2000). Robust Discrete-Time Variable Structure Control Methods, *Journal of Dynamic Systems Measurement, and Control*, 122 (4), 766–775.

Milosavljevic, C., Perunicic-Drazenovic, B. and Veselic, B. (2013). Discrete-time velocity servo system design using sliding mode control approach with disturbance compensation, *IEEE Trans. Ind. Informat.*, 9 (2), 920–927.

Bahn, W., Lee, S., Lee, S., and Cho, D. (2014). Tuningless servo controller using variable structure control and disturbance compensation. *In Proc. of the IEEE International Conference on Industrial Technology*, 96–99, Busan, South Korea.

Han, J., Kim, T., Park, J., Oh, T., Lee, J., Kim, S., Lee, S., Lee, S., and Cho, D. (2017). Gain selection method for robustness enhancement in sliding mode control combined with decoupled disturbance compensator with unknown inertia in industrial servo systems. *17th International Conference on Control, Automation and Systems (ICCAS)*, 1713–1717.

Han, J., Kim, T., Oh, T., Kim, Y., Lee, J., Kim, S., Lee, S., Lee, S., and Cho, D. (2018). Frequency-domain design method for discrete-time sliding mode control and generalized decoupled disturbance compensator with industrial servo applications. *12th IFAC Symposium on Robot Control (SYROCO)*, 96–101.

Wang, G. and Xu, Q. (2018). Sliding mode control with disturbance rejection for piezoelectric nanopositioning control, *In Proc. of American Control Conference (ACC)*, 6144–6149.

Yin, W., Sun, L., Wang, M. and Liu, J. (2018). Robust Position Control of Series Elastic Actuator with Sliding Mode Like and Disturbance Observer, *In Proc. of American Control Conference (ACC)*, 4221–4226.

Huang, J., Wen, C., Wang, W., Jiang, Z. (2013). Adaptive stabilization and tracking control of a nonholonomic mobile robot with input saturation and disturbance, *Systems & Control Letters*, 62 (3), 234–241.

Zhou, J., Cheng, Y., Du, H., Wu, D., Zhu, M., and Lin, X. (2019). Active finite-time disturbance rejection control for attitude tracking of quad-rotor under input saturation, *Journal of Franklin Institute*, accepted.
DOI: 10.1016/j.jfranklin.2019.05.018.

Han, J., Bahn, W., Kim, T., Park, J., Lee, S., Lee, S., and Cho, D. (2016). Decoupled disturbance compensation under control saturation with discrete-time variable structure control method in industrial servo systems. *16th International Conference on Control, Automation and Systems (ICCAS)*, 1453–1457.

Du, J., Hu, X., Krstić, M., and Sun, Y. (2016). Robust dynamic positioning of ships with disturbances under input saturation, *Automatica*, 73, 207–214.

Han, J., Kim, T., Oh, T., Lee, S., and Cho, D. (2020). Effective disturbance compensation method under control saturation in discrete-time sliding mode control, *IEEE Trans. Ind. Electron.*, 67 (7), 5696–5707.